LASER ABLATION IN LIQUID OF GERMANIUM IN EXTERNALLY APPLIED ELECTRIC FIELDS

THESIS IN
Physics

Presented to the Faculty of the University
of Missouri-Kansas City in partial fulfillment of
the requirements for the degree

MASTER OF SCIENCE

By
Yilu Li
B.S. CHANGCHUN UNIVERSITY OF SCIENCE AND TECHNOLOGY, CHINA
2010

Kansas City, Missouri
2013

LASER ABLATION IN LIQUID OF GERMANIUM IN EXTERNALLY APPLIED ELECTRIC FIELDS

Yilu Li, Candidate for the Master of Science Degree

University of Missouri – Kansas City, 2013

ABSTRACT

Laser ablation in liquids has been proven to be an effective path to synthesize nanomaterials.[1] Laser ablation in liquids provides unique advantages since materials are fabricated under nonequilibrium, high-pressure, high-temperature conditions. In addition, it allows for varying many parameters (e.g. laser fluence, liquid) to help control synthesis. Laser ablation in liquids with an externally applied electric field extends the traditional Laser ablation in liquids approach, and in the only published report on this topic, has been shown to control the morphology, size, chemical composition and structure of the samples.[2] In this thesis, the effect of electric fields on Laser ablation in liquids of germanium targets is studied. The aim is to better understand the role of an externally applied electric field in the ablation process and on the ablation products.

Key words: Laser ablation in liquid, Electric field, Germanium, Nanoparticle

APPROVAL

The faculty listed below, appointed by the Dean of the College of Arts and Sciences have examined a thesis titled “laser Ablation in Liquid of Germanium in Externally Applied Electric”, presented by Yilu Li, candidate for the Master of Science degree, and certify that in their opinion it is worthy of acceptance.

Supervisory Committee

Michael Kruger, Ph.D., Committee Chair

Department of Physics

Jerzy M. Wrobel, Ph.D.

Department of Physics

Da-Ming Zhu, Ph.D.

Department of Physics

CONTENTS

ABSTRACT iii

APPROVAL iv

ILLUSTRATIONS vii

TABLES x

ACKNOWLEDGEMENTS xi

Chapter Page

1. INTRODUCTION 1

1.1 Nanomaterials 1

1.2 Laser Ablation Process and Laser Ablation in Vacuum or Air 2

1.3 Laser Ablation in Liquid (LAL) 3

1.4 Electrical Field Assisted Laser Ablation in Liquid 6

1.5 Experimental 7

1.5.1 Excimer Laser 7

1.5.2 Transmission Electron Microscopy. 9

2. EXPERIMENT PROCEDURES 12

2.1 Set up 12

3. FUNDAMENTAL THEORIES 20

3.1 Lambert-Beer-Bouguer Law 20

3.2 Classical Electromagnetic Theory of Laser Reflection 21

3.3 Thermal Mechanisms in Laser Ablation 22

3.4 Energy, Pressure and Particle Generation of Laser Ablation in Liquid 26

4. DATA COLLECTION AND ANALYSIS 29

4.1 Data Collection 29

4.2 TEM Analysis 32

5. CONCLUSION 41

5.1 Conclusion 41

BIBLIOGRAPHY 42

VITA 46

ILLUSTRATIONS

Figure Page

1 Schematic of laser ablation in vacuum/low pressure gas. The laser creates a plasma plume, which expands and cools. Particles in the plume can condense on the surface of the substrate as a thin-film……3

2 (a) Schematic of laser ablation in a liquid. a) An Incident laser beam generates plasma on the target's surface. (b) The plasma plume expands in the liquid, creating a shock and high pressure zone. (c) Chemical reactions may take place inside the plasma and liquid. (d) Condensations of the plasma plume in liquid……4

3 The evolution of the laser-induced plasma in vacuum, air or liquid……...5

4 Energy diagram for a noble gas-halogen gas molecule (dimer). A molecule will remain in the excimer upper level for a short time before releasing a photon and returning to the ground state……...8

5 Photograph of the laser used in this work of excimer laser: COMPexPro 201 F……9

6 A photograph of a TEM grid, which was used to place samples on……9

7 Layout of a basic TEM……..10

8 Container with Ge sample……12

9 Laser intensity control system. Including one zero-order waveplate and two polarizing beamsplitters……13

10 Photograph of system to generate electric fields…….……14

11 Electrodes inside and outside of the container……14

12 a) photograph and b) schematic of the entire system…….....16

13 Laser ablation with ultrasonic vibrator system……17

14 After ablation and preparing for a TEM study. The spot at the center is a TEM grid……...18

15 Quick dry system……18

16 Evaporation process and surface recede velocity V_r, the solid-liquid interface velocity V_{int}……24

17 Sample 1 (With ultrasonic vibrator, No E field, Water)……32

18 Sample 2 (No ultrasonic vibrator, No E field, Water)……32/37

19 Sample 3 (No ultrasonic vibrator, With E field set as 200V, Electrodes outside container)……33

20 Sample 4 (No ultrasonic vibrator, With E field set as 750V, Electrodes outside container)……33

21 Sample 5 (No ultrasonic vibrator, With E field set as 1000V, Electrodes outside container) ……33

22 Sample 6 (No ultrasonic vibrator, With E field set as 1500V, Electrodes outside container, Water)……...34

23 Sample 7 (No ultrasonic vibrator, With E field set as 2000V, Electrodes outside container, Water)……34

24 Sample 12 (No ultrasonic vibrator, With E field set as 18V, Electrodes outside container, Water)……34

25 Sample 8 (No ultrasonic vibrator, With E field set as 18V, Electrodes inside container, Water)……36/37

26 Sample 9 (No ultrasonic vibrator, With E field set as 18V, Electrodes inside container, Water)……36

27 Sample 10 (No ultrasonic vibrator, No E field, Ethanol)……38

28 Sample 11 (No ultrasonic vibrator, With E field set as 18V, Electrodes inside container, Ethanol)……38

29 Measurements of the nanoparticle size for Sample 2, which is no ultrasonic vibrator, no E field and ablated in water……39

30 Particle size – Voltage/Field graph. Shows the relationship between different electric fields and the average particle size……40

TABLES

Table Page

1 Ge Ablation Summary……30

ACKNOWLEDGEMENTS

At the point of finishing this thesis, I would like to express my sincere thanks to who lent me hands in my academic achievements. First of all, I would like to take this opportunity to show my sincere gratitude to my supervisor Dr. Michael Kruger, my mentor and advisor, for his support and guidance throughout my master's program in physics. A special thanks to Dr. Omar Musaev and Dr.Jerzy M. Wrobel for a lot of good advices and precious research experiences during my physics research career. I would also like to thank all committee members for making time for me off their busy schedule. Finally, I appreciate my family members and friends for all their encouragement and support.

Financial support for my studies and research from the UMKC Department of Physics and Astronomy are gratefully acknowledged.

CHAPTER 1
INTRODUCTION

Laser light can have high energy density, small spectral spread, high coherence and high directionality.[2] These features have resulted in lasers being applied in various fields. Because of the high energy carried by laser light, when it is incident on a material's surface the power per unit area transferred from the laser to the materials surface can be very large. This unique energy transfer feature of laser makes it an ideal tool for non-contact micro-processing.[3] By accurately focusing light with a very large energy density, drilling, cutting and welding may be performed.[3]

In many cases, the debris from the interaction of laser light with targets is interesting, often forming nanoparticles. Several papers about formation of nanoparticles by using laser ablation in liquids has been reported within the last decade,[4-7] since then nanoparticles of many materials have been fabricated by ablation of targets in a variety of liquids, for example water,[4, 8] alcohol[8] and liquid nitrogen.[6, 9]

1.1 Nanomaterials

Nanoscale science and technology is a new and challenging scientific field, which was born at the end of 1980s. Its basic aim is to understand nature at the nanoscale (10^{-9}-10^{-7}m), and how to create new substances by controlling atoms and molecules directly.[10]

In the early stages of nanomaterial studies, nanomaterials were confined to nano-thin films and nano-solids constructed by nanoparticles.[10] Today, nanomaterials are

defined in three-dimensional space with at least one dimension in the nano-scale range (1-100nm), or a material constituted by the nano-scale as the basic unit in at least one dimension. According to this classification, different nanomaterials can be divided into different categories. Based on dimensionality, a nanomaterial can be divided into: zero-dimensional (all three dimensions have a nanometer scale), such as nanoparticles, and atomic clusters; one-dimensional (two dimensions are of the nanometer scale), such as nanowires, nanorods, and nanotubes; and two-dimensional (one dimension has a nanometer scale), such as ultra-thin films, multilayers, and super-lattices. The nanometer dimensions typically result in quantum effects being prominent, so the divisions are often referred to in a manner that highlights this, with 0-D being referred do as quantum dots, 1-D as quantum wires and 2-D as quantum traps.[11]

1.2 Laser Ablation Process and Laser Ablation in Vacuum or Air

Laser ablation is a process that uses laser beams to remove material from a solid surface. The ablation process can roughly be divided by laser flux, into a low and a high flux level. For a low laser flux ($\leq 2 \times 10^{13}\ \mathrm{W/cm^2}$)[12], the target surface is rapidly heated resulting in sublimation and evaporation. This is used in industry for making thin-films, such as generating $YBa_2Cu_3O_{7-\delta}$ thin-films and is a way to investigate the effects of the oxygen pressure and laser energy on the angular distribution of deposited species.[13-15] For high flux levels ($\geq 2 \times 10^{13}\ \mathrm{W/cm^2}$), which was used in this study, the laser radiation converts some of the target material into a plasma.[16]

During a sufficiently intense laser pulse, the laser energy that is absorbed by the target surface, causes material to be removed from the surface.[1] The material is converted into plasma, which if the pulse is sufficiently long, will absorb a part of the energy from laser beam too. The ejected material then expands outward from the target surface. This expansion of the laser-induced plasma is a free expansion, when laser ablation occurs in vacuum or a low-pressure gas. At the end of the pulse, the heat radiates and is conducted away, and the plasma rapidly cools.[17] While the temperature of the plasma drops, the plasma condenses to a solid form. Condensation typically takes two forms. A substrate may be placed near the ablated surface and the ablated material can coat the substrate forming a thin film as Figure 1.[13], In addition, the plasma can condense in a buffer gas forming nanoparticles.[16, 18]

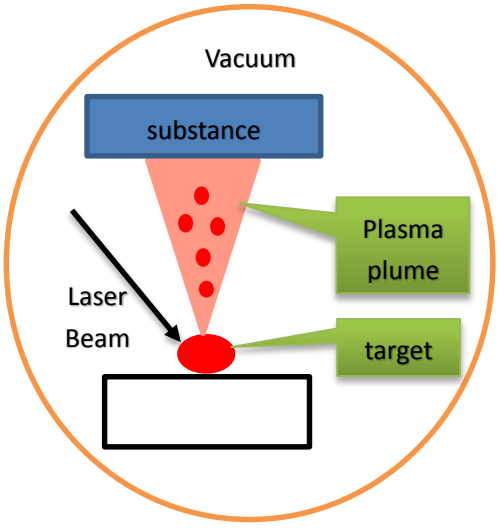

Figure 1 Schematic of laser ablation in vacuum/low pressure gas. The laser creates a plasma plume, which expands and cools. Particles in the plume can condense on the surface of the substrate as a thin-film.

1.3 Laser Ablation in Liquid

In 1987, Patil performed the first experiment involving laser ablation in a liquid.[19]

He used a pulsed ruby laser to ablate an iron target in water, which created a metastable phase of iron oxide.[19] However, that is just one of the first reports of laser ablation in liquid, and the formation of nanoparticles under laser ablation of solids in liquid environments has subsequently received a fair degree of study.[4]

Although the first work on laser ablation in liquids was in 1987, it was not until the late 1990s that researchers placed a greater emphasis on using laser ablation in

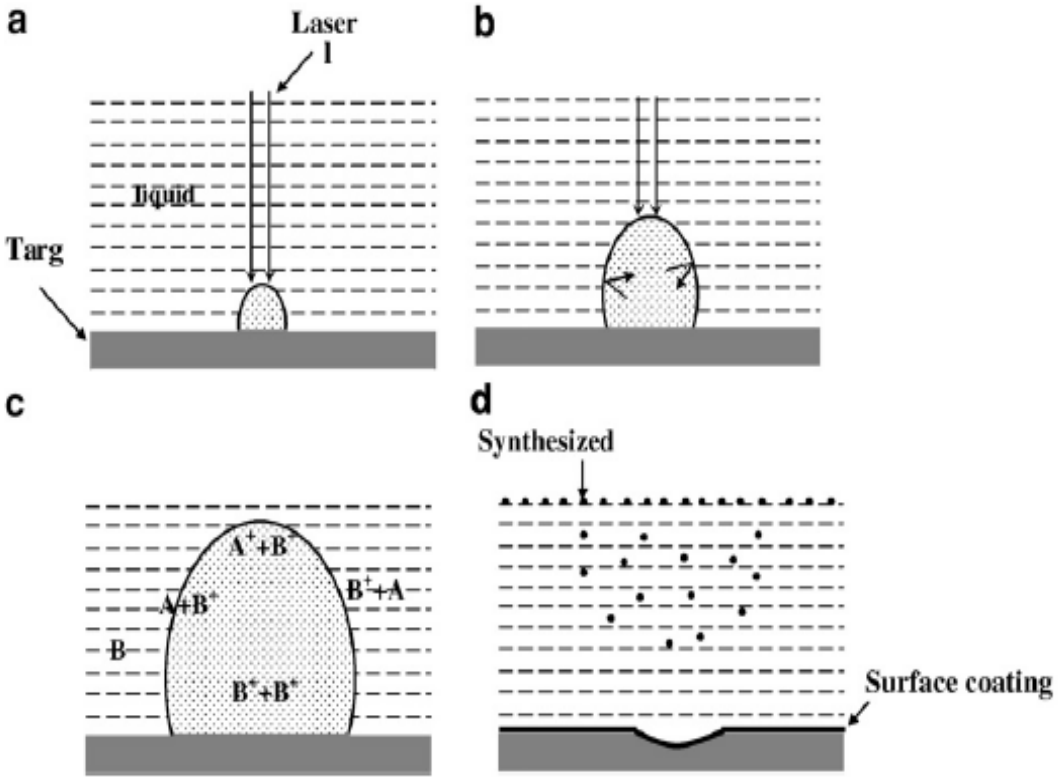

Figure 2 Schematic of laser ablation in a liquid. a) An Incident laser beam generates plasma on the target's surface. (b) The plasma plume expands in the liquid, creating a shock and high pressure zone. (c) Chemical reactions may take place inside the plasma and liquid. (d) Condensations of the plasma plume in liquid.
G.W. Yang. (2007). Progress in Materials science [Laser Ablation]. GuangZhou, China; Zhongshan University.[1]

liquids as a means to synthesize nanomaterials.[4, 16, 20] When a high intensity laser beam interacts with a target immersed in a liquid both the solid target and nearby liquid

are heated rapidly. The plasma plume will appear near the solid-liquid interface, which is called a laser-induced plasma plume. Unlike the free expansion of the plasma plume from laser ablation in vacuum or low pressure gas, the plasma plume expansion process produces a shock wave in the liquid, because the surrounding liquid confines its expansion. The shock wave induces pressure inside of the laser-induced plasma plume. Within this plasma plume a high temperature and high pressure zone is produced. This region provides an extreme environment for chemical reactions taking place inside the plasma and liquid, as well as their interface. These extreme, metastable conditions may also provide the right circumstances to fabricate new materials, possibly by combining of the elements of the target and liquid.

When a laser pulse decays, the plasma cools and the pressure decreases as shown

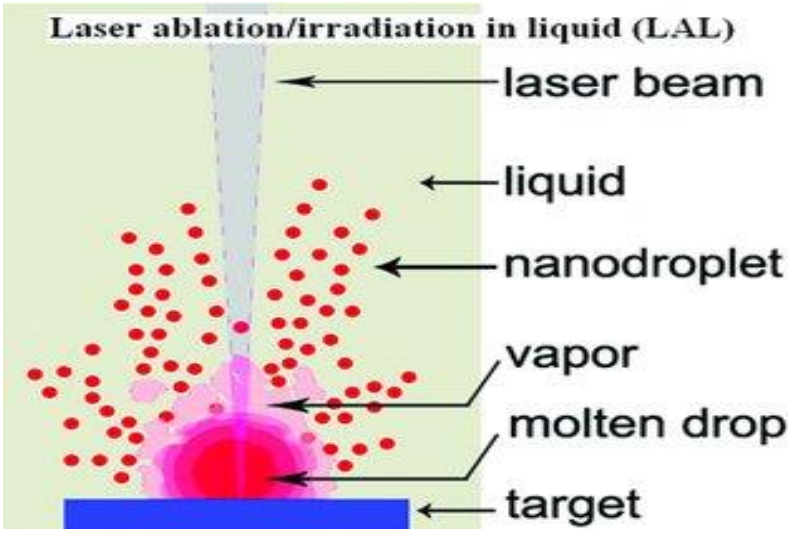

Figure 3 The evolution of the laser-induced plasma in vacuum, air or liquid. Haibo Zeng, Xi-Wen Du, Subhash C.Singh, Sergei A. Kulinich, Shikuan Yang, Jianping He, Weiping Cai. (2012). Advanced Functional Materials. [Nanomaterials]. Hefei, China. Chinese Academy of Sciences.[1]

in Figure 3. Atoms will aggregate with other, nearby atoms, and subsequently combine to form clusters of atoms, which may then grow to nano-sized particles.

Similar to laser ablation in vacuum or a gas, laser ablation in liquids can be used to fabricate nanoparticles or thin films. Laser ablation in liquids has proven to be a novel method for material fabrication. For example, in 1993, Niu, used laser ablation to synthesis carbon nitride by ablating graphite targets in liquid nitrogen,[9] while in 2013, Hamidi used laser ablation in liquid technique to synthesize magneto-optical cobalt thin films by electron beam deposition onto the Ag nanoparticles.[21]In short, laser ablation in liquids of solid targets is a relatively new method to fabricate nanocrystals.[22]

Comparing laser ablation in vacuum or gases with laser ablation in liquids, one finds the main difference between these two methods is a much shorter free path of the ablated species in the latter case.[4] For laser ablation in vacuum or gas, the synthesized nanoparticles rapidly leave the laser beam and might be stick on the system chamber, but for laser ablation in a liquid, nanoparticles might be return into the laser beam again during their motion for further processing, unless care is taken to prevent that from happening.

1.4 Electrical Field Assisted Laser Ablation in Liquid

There has been interest in using externally applied electric and magnetic fields for laser ablation in vacuum and low-pressure gases. When scientists ablated a Zn target in an electric field, the concentrations of electrons excited and ionic species in the laser-induced plasma plume, as well as its kinetic energies, were found to be strongly dependent on the bias voltage applied to the target.[23] Also, the preparation of thin films, for example $SrBi_2Nb_2O_9$, by laser ablation in vacuum system with external electric field

assist is also popular,[15, 24] because of it is easy to construct of the system and also high efficiency, high purity for the thin-film deposition.

Due to the interesting results found when laser ablation in vacuum occurs in the presence of an externally applied electric field, one would expect similarly interesting results from laser ablation in liquids in the presence of externally applied electric fields. To date there has been just one publication on this topic, which is why it is being further investigated in this thesis. [25]

1.5 Experimental

1.5.1 Excimer Laser

Excimer lasers are a type of pulsed gas laser, with wavelengths in the ultraviolet region. The first excimer laser was invented in 1970 by Nikolai Basov, V. A. Danilychev and Yu. M. Popov in Moscow.[26] They used a strong electron beam to excite liquid xenon dimers, which then underwent stimulated emission at 172 nm.[26] As a gas laser, the working gas for an excimer laser consists of inert gas atoms (e.g. Ne, He, Ar, Kr, Xe) and halogen atoms (F, Cl, Br, etc.).[2] Although noble gas atoms can react with halogen atoms, the molecules are short lived and exist in only in excited electronic states with the ground level consisting of separate atoms. There is no stable ground level, which is shown schematically in Figure 4.

When an excited molecule makes a transition from the upper level bound state to the ground state, it quickly (10^{-13} s) dissociates into unbound atoms and release a photon. Because of the very short period of such molecules in the excited state, it had been

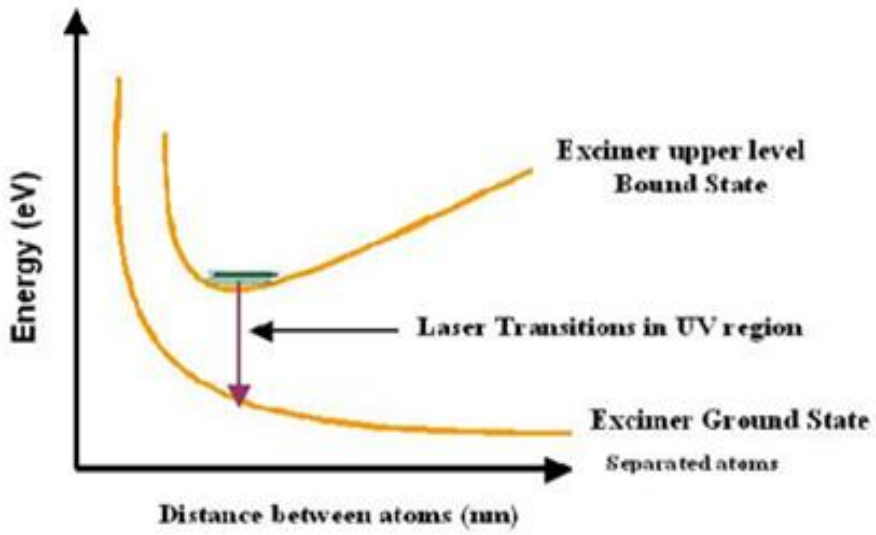

Simplified energy level diagram of Excimer laser

Figure 4 Energy diagram for a noble gas-halogen gas molecule (dimer). A molecule will remain in the excimer upper level for a short time before releasing a photon and returning to the ground state.
http://www.worldoflasers.com/lasertypes2.htm

named "excimer" from the phrase excited dimer.[2] Excimer lasers, which can have high intensities and are pulsed, are used in many fields such as medicine, scientific research and industrial applications.[25, 27-29]

For this experiment, we used a Coherent COMPexPro 201F excimer laser, which is shown in Figure 5. The active medium in this excimer laser is a mixture of a rare gas, a halogen gas and a buffer gas. The mixture gas is F_2 in He / Xe / Ne / He. The wavelength is 351 nm, the beam has a pulse duration is 25 ns, a maximum pulse energy of 300 mJ, and the repetition rate is 1-10Hz.

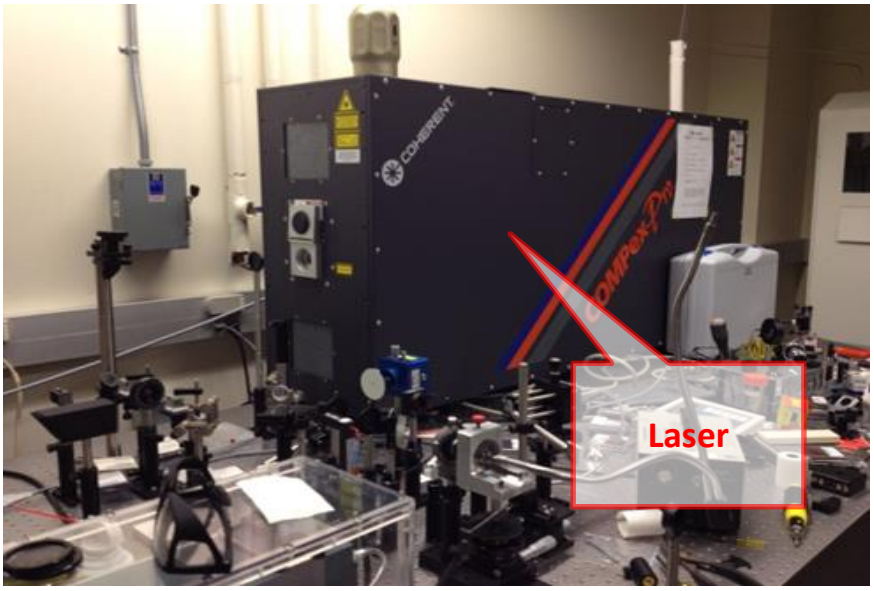

Figure 5 Photograph of the laser used in this work of excimer laser: COMPexPro 201 F.

1.5.2 Transmission Electron Microscopy.

The first transmission electron microscope (TEM) was built by Max Knoll and Ernst Ruska in 1931.[30] A transmission electron microscope takes advantage of the wave nature of electrons to image very thin samples.[31, 32] An accelerated electron beam generated by electron gun is accelerated and passes through a thin sample held in place by a grid (Figures6).

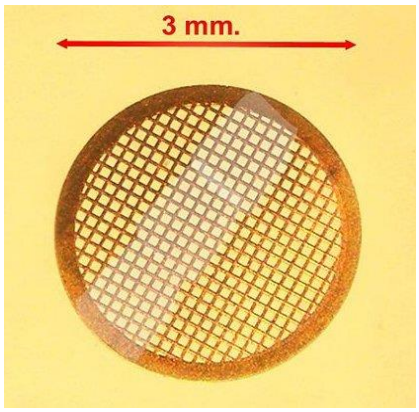

Figure 6 A photograph of a TEM grid, which was used to place samples on. http://commons.wikimedia.org/wiki/File:Retino_ME_con_sezioni.jpg

The objective lens forms an image of the electron density distribution, which is related to the thickness, composition and structure of the specimen. The diffraction, intermediate and projector lenses are used to focus and magnify this image onto a fluorescent screen. Since the electron de Broglie wavelength is small, the resolution of a TEM can reach down to 0.1nm. The diagram outlining the internal components of a basic TEM system show as Figure 7. For my thesis project, I received help from Dr.

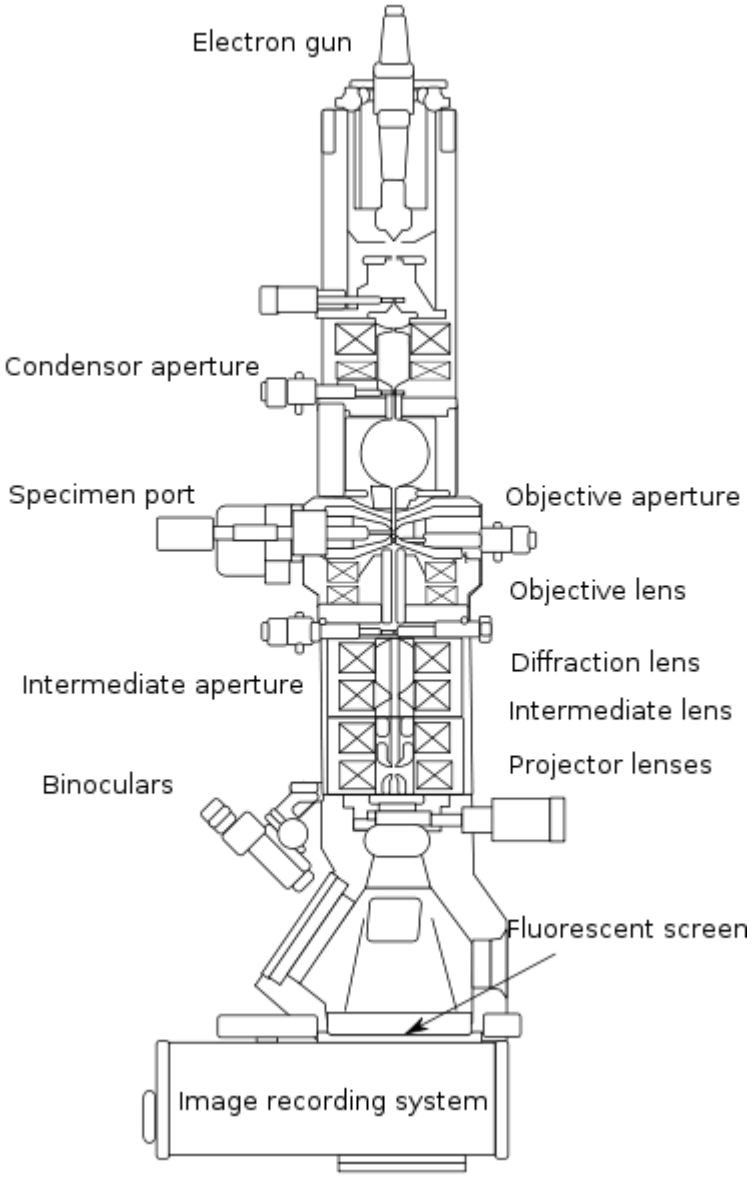

Figure 7 Layout of a basic TEM.
http://en.wikipedia.org/wiki/File:Scheme_TEM_en.svg

Vladimir Dusevich, who is from the UMKC-School of Dentistry. The machine he used is a Scanning Transmission Electron Microscope CM12. The high voltage range is from 20 to 120kV; the electron gun is using a lanthanum hexaboride source (LaB6) and magnification is from 70X to 510000X.

CHAPTER 2

EXPERIMENT PROCEDURES

2.1 Set up

A rectangular glass cell, which has two polished windows and an open top was used to contain the liquid (distilled water or ethanol) and the sample. The container dimensions are $5.0 \times 5.0 \times 2.0\ cm^3$. The germanium sample was glued on a stage, which was made by a plastic tie, and attached to the two edges of the container as shown in Figure 8. The reason for using a plastic tie as a stage for the target is because this way we could suspend the sample in the desired location.

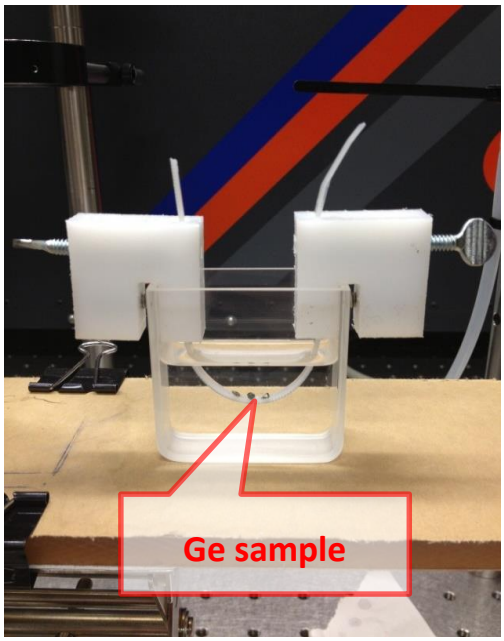

Figure 8 Container with Ge sample.

In our project, we used an ultra violet (UV) excimer laser, with a wavelength of 351 nm. Using a lens we narrowed the width of our pulsed UV light spot down to micron level (≈6μm). This provides sufficient condition for nanoparticles production.

When the laser beam was incident on the sample, it not only generated nanoparticles, but also broke off some large chunks of the sample. If we glued the

sample at the bottom of the container, the large broken off pieces would occasionally block the laser. With the sample suspended, these large pieces, which fell to the bottom of the container, would not influence the result.

After setting up and warming up of the excimer laser, the experiment was ready to be run. The laser was set for a frequency of 2 Hz and the beam energy for 125 mJ. Two polarizing beamsplitters and one 351nm zero-order half- waveplate, which was set for

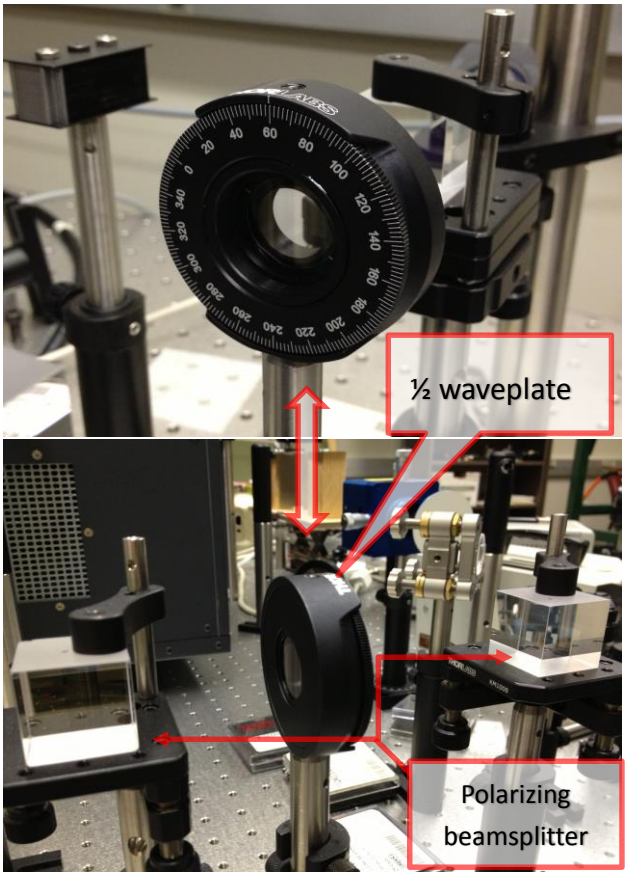

Figure 9 Laser intensity control system. Including one zero-order waveplate and two polarizing beamsplitters.

20 degree, were used to vary the laser fluence, as shown in Figure 9. The combination of the half-waveplate, and two polarizing beamsplitters allows one to control the laser fluence.

To produce the electric field, we used two wood stages, which supported two metal plates, as shown in figure 10. We placed them on either inside (the electrodes

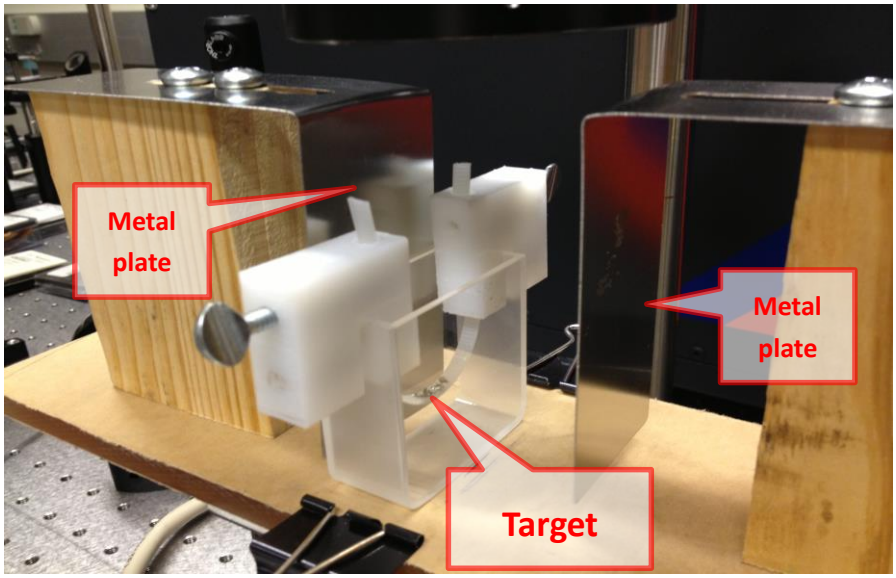

Figure 10 Photograph of system to generate electric fields.

attached the internal surfaces of the container means the electrodes are in the liquid) or outside (the electrodes are attached the external surface of the container) of the liquid filled container as figure 11.

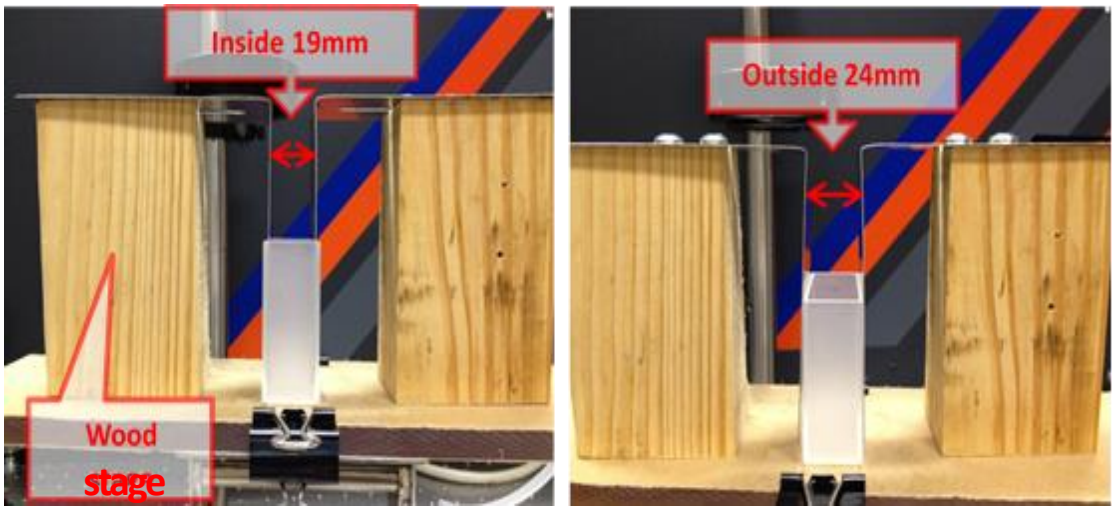

Figure 11 Electrodes inside and outside of the container

For all experiments, we made sure the two plates were parallel (by using a ruler to measure the distance of both the left and right sides to make sure they were separated by the same amount). The distance between the plates was 1.9 cm when the plates are

inside of the container, and 2.4 cm when they were outside of the container. These plates were connected to a power supply, which was set to five potential differences 0 V, 5 V, 10 V, 15 V, 18 V, which corresponded to electric fields of 0 V/cm, 2.63 V/cm, 5.26 V/cm, 7.89 V/cm, and 9.47 V/cm when the plates were inside of the container. An variable static electric field could be created after adjusting all of above, and then connecting the electric clips to the electrodes and power supply. The entire system, except for the power supply, was mounted on an adjustable stage, therefore, the target could be brought to the focal point of the lens.

The whole system as shown below in Figure 12:

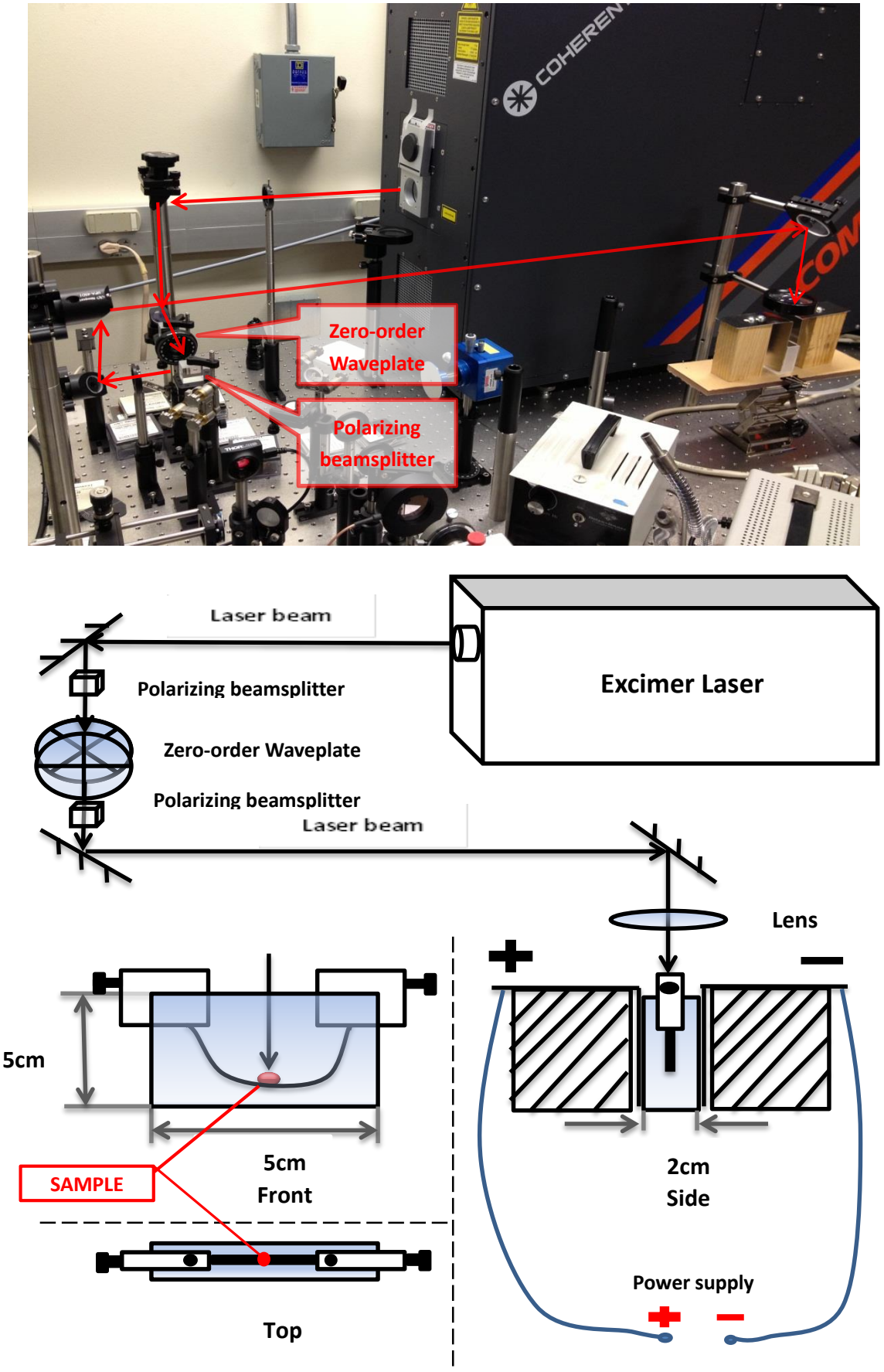

Figure 12 a) photograph and b) schematic of the entire system.

In the experiment, I also used an ultrasonic vibrator (Figure 13a) for the system. So, the system has a little changes with the ultrasonic vibrator has been provided (Figure 13b). A plastic cup has been used to instead of the glass container for the laser ablation. The plastic cup was fixed by a metal suspender. And two electrodes were fixed at the edge of the plastic cup and also for the plastic band, which hold the Ge sample (Figure 13c).

Figure 13 Laser ablation with ultrasonic vibrator system

a. Ultrasonic vibrator

b. LAL with Ultrasonic vibrator system

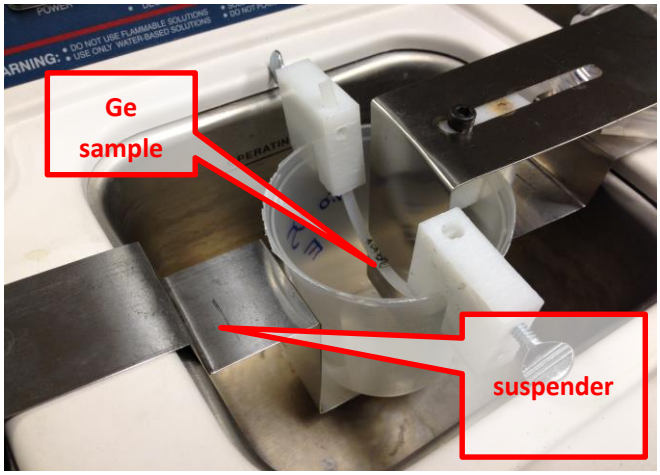

c. Set up of Ultrasonic vibrator system

The final step was to run the laser for 30 minutes. After ablation, we poured the liquid from the experimental container to a clean plastic cup and then placed a TEM grid into the plastic cup (Figure 14), and put the cup into a fume hood. Typically, after

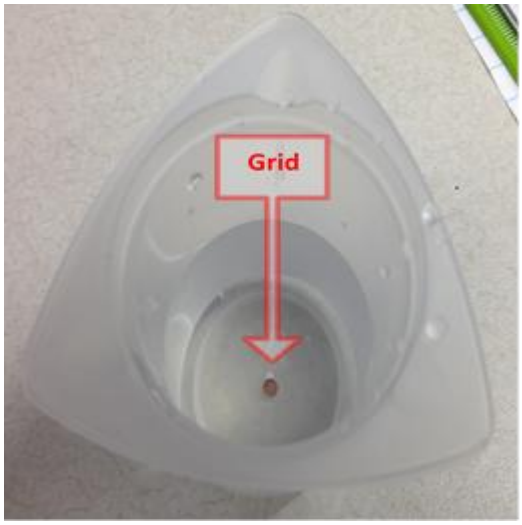

Figure 14 After ablation and preparing for a TEM study. The spot at the center is a TEM grid.

four days the liquid in the cup would have evaporated with the room temperature. Also, in order to figure out whether there is an influence between different drying ways, a new 60 ^{o}C drying system has been provided as following (Figure 15):

Figure 15 Quick dry system

I used one hotplate, which could control temperature, as my heating source. Putting a metal cup on the hotplate and another glass beaker which filling the sample liquid (after ablation and volume is around 20ml) had been put inside of the metal cup as above Figure 15 shown. Then set the temperature to 60 Celsius degrees. This system could make the drying time short to several hours.

These procedures were repeated with different voltages and electrodes were set both inside and outside of the liquids (ethanol and distilled water).

CHAPTER 3

FUNDAMENTAL THEORIES

3.1 Lambert-Beer-Bouguer Law

Laser ablation is an energy transfer process and as such must follow the law of conservation of energy. When the laser beam interacts with materials, the energy carried by the laser light follows the equation:

$$1 = \frac{E_r}{E_0} + \frac{E_a}{E_0} + \frac{E_t}{E_0} = R + \alpha + T \tag{3.1}$$

where R is the reflection coefficient; α is the absorption coefficient; and T is the transmission coefficient of the material. For an opaque material, E_t=0 equation (3.1) changes to:

$$1 = R + \alpha \tag{3.2}$$

If I is the laser intensity and dI is the reduction of the intensity as the light passes through a thickness of target, dx, then

$$\mathrm{dI}/\mathrm{I} \propto \mathrm{dx}, \text{ thus } \frac{\mathrm{dI}}{\mathrm{I}} = -\alpha \mathrm{dx} \tag{3.3}$$

$$\alpha = \sigma \mathrm{N} \tag{3.4}$$

Where the proportionality constant α, is known as the absorption coefficient, σ, is the absorption cross section, and N is the number density of the absorbers.

Consider a laser beam incident on a surface with an intensity I_0, Integrating equation 3.3 from 0 (surface) to a depth x below the surface yeilds[2]:

$$\mathrm{I} = I_0 e^{-\alpha x} \tag{3.5}$$

Equation (3.5) is known as the Lambert-Beer-Bouguer Law and shows that as light passes through a material it is absorbed exponentially, as a function of travelled distance.

3.2 Classical Electromagnetic Theory of Light Reflection

Within the laser ablation in liquid method, because of the laser beam went through the liquid first then going into the target material. Therefore, not only absorption exists, but also reflection.

Laser light is an electromagnetic wave, which means one may use following equations to describe the speed of its propagation in a medium:

$$n^2 = \frac{\mu}{2}\left[\sqrt{\varepsilon^2 + \left(\frac{4\pi\sigma}{\omega}\right)^2} + \varepsilon\right] \tag{3.6}$$

where n is the index of refraction of the material (n=c/v). The electric field of laser light in the medium is E, its frequency is ω, the permittivity of the medium is ε, its magnetic permeability is μ, and its conductivity is σ. The complex refractive index is $\hat{n}$ ($\hat{n}$ =n-iκ) and it reflects the time delayed phase compensation. κ is the extinction coefficient related to the attenuation of electromagnetic wave amplitudes.[33, 34]

Because $\hat{n}$ =n-iκ, we can ascertain:

$$\kappa^2 = \frac{\mu}{2}\left[\sqrt{\varepsilon^2 + \left(\frac{4\pi\sigma}{\omega}\right)^2} - \varepsilon\right] \tag{3.7}$$

For dielectric materials, σ=0, n^2=με>1 and κ=0 shows the propagation velocity of the laser light in a purely dielectric medium is slower than light speed in a vacuum, and its intensity attenuates also.

From section 3.1, we already know that α is the linear absorption coefficient, which α can be shown as follows:

$$\alpha = \frac{2\omega\kappa}{c} = \frac{4\pi\kappa}{n\lambda} = \frac{4\pi\kappa}{\lambda_0} \tag{3.8}$$

In formula 3.7, λ and λ_0 indicate the wavelength of laser light in the medium and

vacuum, $\omega\lambda_0 = 2\pi c$. The depth of absorption for the medium can be presented as $1/\alpha = \delta$, so δ shows the distance of light intensity as it decays.[33, 34] In this case, the laser light is at normal incidence, using superscripts i, r and t as the incidence, reflection and refraction of light beams. The propagation distance of reflection and refraction at the interface is zero, no phase postponed, so only the wave amplitude need be considered. Using Maxwell equations to export normal incidence:

$$E_0^r = \frac{\hat{n} - \mu}{\hat{n} + \mu} E_0^i \; ; \; E_0^t = \frac{2\mu}{\hat{n} + \mu} E_0^i \tag{3.9}$$

The ratio of intensity of reflected light and the incident beam is called reflectance R:

$$\mathrm{R} = \left| E_0^r / E_0^i \right|^2 = \frac{(n-\mu)^2 + \kappa^2}{(n+\mu)^2 + \kappa^2} \tag{3.10}$$

Usually, $\mu \approx 1$, in the dialectics:

$$\mathrm{R} \approx (n-1)^2/(n+1)^2 \tag{3.11}$$

Electromagnetic theory also shows the relationship between light absorption and reflectance for the same object are a proportional relationship[34]. While the laser beam passed through the medium 1 and became incident on medium 2, the reflectance at the interface of these two media is:

$$\mathrm{R} = \frac{(n_1 - n_2)^2 + (\kappa_1 + \kappa_2)^2}{(n_1 + n_2)^2 + (\kappa_1 - \kappa_2)^2} \tag{3.12}$$

In this project, the laser beam went through water or ethanol, and then reached a germanium target. So medium 1 is the refractive index of water or ethanol, and medium 2 is the refractive index of germanium: n_{water}=1.34, $n_{ethanol}$=1.37, $n_{germanium}$=4.02.

3.3 Thermal Mechanisms in Laser Ablation

The thermal mechanisms of laser ablation includes surface evaporation, melting

and phase explosion.[16]

The following equation describes the heat flow for a simplified one-dimensional model for the evaporation and melting of a metal surface [16, 35]:

$$c(T)\rho(T)\frac{\partial T}{\partial t} = \frac{\partial}{\partial x}\left(K(x,T)\frac{\partial T}{\partial x}\right) + \alpha I(x,t) \tag{3.13}$$

Where T is the temperature, x is the deepness and t is the time; *I* is the absorbed laser intensity as Lambert-Beer-Bouguer Law shows; c , ρ and K the thermal capacity, density and thermal conductivity of the target material. For simplicity ρ and K are frequently assumed to be temperature and space independent.[16]

When surface melting takes place, the solid-liquid phase transition must be considered. To consider this transition during laser irradiation, two boundary conditions are required at the interface where the phase transition occurs. Combining the boundary conditions with conservation of energy ($J = -K\nabla T$) results in [16]:

$$\rho\Delta H_m(T_{tr})v_{int} = K_{solid}\left.\frac{\partial T}{\partial x}\right|_{x^+ int} - K_{liquid}\left.\frac{\partial T}{\partial x}\right|_{x^- int} \tag{3.14}$$

Where T_{tr} is the transition temperature; K_{solid} is the thermal conductivity of the solid phase; K_{liquid} is the thermal conductivity of the liquid phase; ΔH_m is the heat of fusion at $T=T_{tr}$; v_{int} is the velocity at the solid-liquid interface, which should be a function of $T_{tr} - T_m$, and T_m is the melting temperature, which can be written generally as [16]:

$$v_{int} = f(T_{tr} - T_m) \tag{3.15}$$

Due to surface evaporation, the target's surface recedes at a velocity v_r as shown in figure 16). Suppose a reference frame is positioned such that the target's surface is

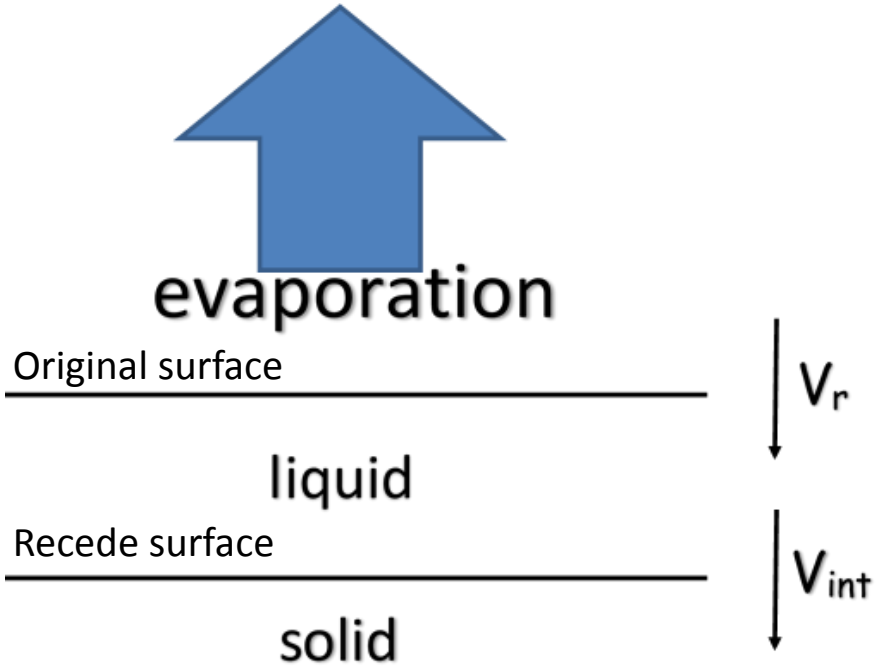

Figure 16 Evaporation process and surface recede velocity V_r, the solid-liquid interface velocity V_{int}

at x=0. The temperature dependence equation (3.13) then becomes[16]:

$$c\rho \frac{\partial T}{\partial t} = K \frac{\partial^2 T}{\partial x} + c\rho v_r \frac{\partial T}{\partial x} + \alpha I(x,t) \tag{3.16}$$

To compute v_r to consider that liquid is in thermal equilibrium with its saturated pressure. If N_v is the number of the particles evaporating per unit time and area then[16,35]:

$$N_V = \frac{p}{(2\pi kTm)^{1/2}} C_s \tag{3.17}$$

Where p is the gas pressure and C_s is the sticking coefficient.[16]

For high intensity pulses, phase explosion will occur when temperature rises at a rate of ~10^9 K/s. At this point, the melted layer on the target surface transfer from a stable state into a metastable state. In the vicinity of critical temperature of ~0.9 T_c, homogeneous nucleation causes: intensive bubble formation, energy release, and formation of a foam consisting from liquid droplets and vapor.[36] This explosive process

is also called phase explosion, where the rate of homogeneous nucleation increase in a short period of time.[35,36] In other words, the temperature of the liquid becomes higher than that of vaporing under the given pressure. This increase causes shifts from the bimodal states into the metastable states. If the target of laser ablation experiment is a metal, the relationship between vapor pressure and temperature is an equilibrium surface process. From the Clausius-Clapeyron equation one may derive:

$$\ln(\frac{p_1}{p_2}) = \frac{\Delta H_{vap}}{R}(\frac{1}{T_2} - \frac{1}{T_1}) \tag{3.18}$$

This relation shows a discontinuous phase change between two phases.[16, 37] Where P_1 and P_2 are the pressures at two temperatures T_1 and T_2, and R is the universal gas constant. In laser ablation in liquid equation (3.18) changes to:

$$p_s = p_0 exp\left(\frac{H_{vap}(T-T_b)}{RTT_b}\right) \tag{3.19}$$

T is the surface temperature and p_s is the vapor saturation pressure; p_0 is the ambient pressure; H_{vap} is the enthalpy of vaporization and T_b is the equilibrium liquid-vapor temperature at the ambient pressure.[35, 36] This equation represents the equilibrium between the surface temperature T and the vapor saturation pressure p_s.

Once in the metastable region a liquid not need to reach the spinodal line to change into a liquid-vapor mixture. A process which will prevent a liquid from reaching the spinodal line is called homogeneous nucleation. It consists of the spontaneous creation of vapor nuclei within the liquid, without the aid of pre-existing nucleation sites. Spontaneous nucleation prevents significant superheating resulting in the liquid changeing into a mixture of gas and droplets.[35] The rate of spontaneous nucleation is given by[36]:

$$J = N\left(\frac{31\sigma}{\pi m}\right)^{1/2} exp\left(\frac{-W_{cr}}{k_B T}\right) \quad (3.20)$$

W_{cr} is the energy needed to form critical vapor cluster at temperature T ; N is the number of liquid molecules per unit volume as equation (3.17) and σ is the surface tension.[36]

From the perspective of nanoparticle formation, an important factor is the time that it takes for a vapor to grow into a cluster. This period of time is named time lag and must be considered when studying laser ablation. Equation 3.20 can be modified to account for this time lag τ[36]:

$$J = N\left(\frac{3\sigma}{\pi m}\right)^{1/2} exp\left(\frac{-W_{cr}}{k_B T}\right) exp\left(\frac{-\tau}{t}\right) \quad (3.21)$$

where t is the time duration for liquid heated; $\tau \approx \left(\frac{2\pi M}{RT}\right)^{1/2} \frac{4\pi\sigma P_S}{(P_S - P_0)^2}$; and M is the molar weight of the substance. [36]

3.4 Energy, Pressure and Particle Generation of Laser Ablation in Liquid

At the beginning of laser ablation, the target absorbs the laser energy. Then, a plasma plume is created at the liquid-solid interface and a shock wave is generated at the solid-liquid interface and moves through the liquid. For long enough pulses, some of the laser energy is also absorbed by the generated laser plasma and transformed into its internal energy E_i.[17] Thus, the laser intensity obeys the following equation[17]:

$$I(t) = P(t)\frac{dL(t)}{dt} + \frac{d[E_i(t)L(t)]}{dt} \quad (3.22)$$

The shock wave creates a high pressure and high temperature zone, where P is the pressure of the plasma plume; L is the length of the plasma plume; and E_i is the internal energy of the plasma. Also E_i presented as a sum of the thermal energy $\sum E_{th} = \alpha E_i$, here α determines the energy fraction transferred to the thermal energy of the plasma. Two

equations[17] show the pressure and length for the beginning of laser ablation in a liquid (τ is the laser pulse):

$$P_0 = P(\tau) = \sqrt{\frac{\alpha}{2\alpha+3} Z I_0} \tag{3.23}$$

$$L_0 = L(\tau) = \frac{4\tau}{3} \sqrt{\frac{\alpha}{2\alpha+4} \frac{I_0}{Z}} \tag{3.24}$$

When the plasma plume expansion in the confining liquid environment, time becomes a reactions for both pressure and length

$$P(t) = P_0 \left[1 + \frac{\gamma+1}{\tau}(t-\tau)\right]^{-\gamma/\gamma+1} \tag{3.25}$$

$$L(t) = L_0 \left[1 + \frac{\gamma+1}{\tau}(t-\tau)\right]^{1/\gamma+1} \tag{3.26}$$

where γ=1+2α/3, is adiabatic parameter of the plasma plume.[17] The plasma plume density is higher at the end of a pulse than the beginning while the temperature is lower at the end than at the beginning. These changes lead to the formation of the nanoparticles, and the particle size is controlled by the free energy [17]:

$$\Delta G(n, c) = -nkT\, ln\,(c/c_0) + 4\pi a^2 n^{2/3} \sigma \tag{3.27}$$

Where k is the Boltzmann constant; T is the temperature in Kelvin; a is the effective radius of plume species (in this case, it is germanium atoms); c is the concentration of atoms; c_0 is the equilibrium concentration of atoms; and σ is the effective surface tension (in this case liquid germanium).[17] It should be noted that the plasma plume not only results in nanoparticles of the target materials but can also result in nanoparticles of combination of the target and liquid. The rate of production of clusters is show as below[17]

$$\rho(t) = 4\pi a n_c^{1/3} D c^2 \exp[\frac{-\Delta G(n_c, c)}{kT}] \tag{3.28}$$

Where D is the diffusion coefficient of germanium atoms in the liquid, D=kT/6πησ

where η is the viscosity $\eta = A \cdot 10^{B/(T-C)}$. For water, $A = 2.414 \times 10^{-5}$ Pa s, B=247.8K, and C=140K[17]; for ethanol, $A = 1.074 \times 10^{-3}$ Pa s, B=298.15K, and C=150K.[38]

CHAPTER 4

DATA COLLECTION AND ANALYSIS

4.1 Data Collection

We ablated germanium under many different configurations of liquids and electric fields. This is summarized in the Table 1.

Table 1 Ge Ablation Summary

	Liquid	Voltage (V)	E field (V/cm)	Electrode	US*	Dry*	EDS*	SEM*	TEM*
1	WATER	NA	0	NA	Yes	RT*	NA	NA	Filaments complex network (a mess)
2	WATER	NA	0	NA	NA	RT*	NA	NA	100nm spheres with some spider web
3	WATER	200	90.9	Outside	NA	RT*	NA	NA	Messy network and no obvious changes
4	WATER	750	340.9	Outside	NA	RT*	NA	NA	
5	WATER	1000	454.55	Outside	NA	RT*	NA	NA	
6	WATER	1500	681.81	Outside	NA	RT*	NA	NA	
7	WATER	2000	909.09	Outside	NA	RT*	NA	NA	
8	WATER	18	9.47	Inside	NA	RT*	Yes	Yes	30nm nanoparticles
9	WATER	18	9.47	Inside	NA	60 °	NA	NA	Some crescent
10	ETHANOL	0	0	Inside	NA	RT*	Yes	Yes	200nm nanoparticles
11	ETHANOL	18	9.47	Inside	NA	RT*	Yes	Yes	90nm nanoparticles
12	WATER	18	8.18	Outside	NA	RT*	NA	NA	messy network
13	WATER	0	0	Inside	NA	RT*	NA	Yes	100nm nanoparticles
14	WATER	5	2.63	Inside	NA	RT*	NA	Yes	Messy network
15	WATER	10	5.26	Inside	NA	RT*	NA	Yes	Messy network
16	WATER	15	7.89	Inside	NA	RT*	NA	Yes	Messy network
17	WATER	18	9.47	Inside	NA	RT*	NA	Yes	Messy network
18	ETHANOL	0	0	Inside	NA	RT*	NA	NA	116nm nanoparticles
19	ETHANOL	5	2.63	Inside	NA	RT*	NA	NA	110nm nanoparticles
20	ETHANOL	10	5.26	Inside	NA	RT*	NA	NA	105nm nanoparticles
21	ETHANOL	15	7.89	Inside	NA	RT*	NA	NA	100nm nanoparticles
22	ETHANOL	18	9.47	Inside	NA	RT*	NA	NA	Messy network

	Liquid	Voltage (V)	E field (V/cm)	Electrode	US*	Dry*	EDS*	SEM*	TEM*
23	WATER	0	0	Inside	NA	RT*	NA	NA	103nm nanoparticles
24	WATER	5	2.63	Inside	NA	RT*	NA	NA	Messy network
25	WATER	10	5.26	Inside	NA	RT*	NA	NA	Messy network
26	WATER	15	7.89	Inside	NA	RT*	NA	NA	Messy network
27	WATER	18	9.47	Inside	NA	RT*	NA	NA	35nm nanoparticles
28	WATER	0	0	Inside	NA	RT*	NA	Yes	Messy network
29	WATER	5	2.63	Inside	NA	RT*	NA	Yes	92nm nanoparticles
30	WATER	10	5.26	Inside	NA	RT*	NA	Yes	65nm nanoparticles
31	WATER	15	7.89	Inside	NA	RT*	NA	Yes	35nm nanoparticles
32	WATER	18	9.47	Inside	NA	RT*	NA	Yes	Messy network

* US means Ultra sonic vibrator
Dry means drying temperature
RT means room temperature
EDS means Energy-dispersive X-ray spectroscopy
SEM means Scanning Electron Microscope
TEM means Transmission Electron Microscope

4.2 TEM Analysis

After completing the ablation experiments that are summarized in the previous table we collected TEM images and analyzed them.

First compare samples 1(Figure 17) & 2(Figure 18), both with no externally applied electric field, but the difference is with or without ultrasonic vibrator.

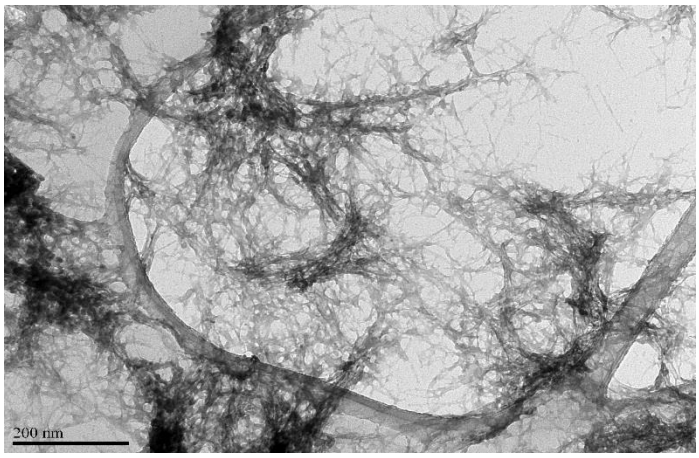

Figure 17
Sample 1
With ultrasonic vibrator
No E field
Water

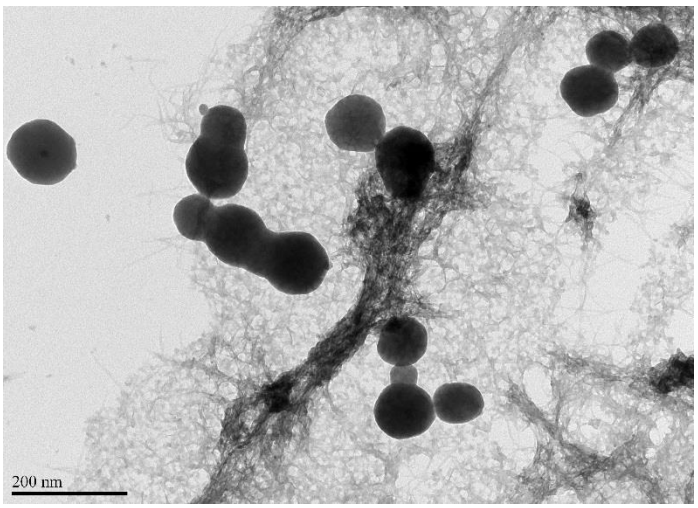

Figure 18
Sample 2
No ultrasonic vibrator
No E field
Water

both images show complex networks, but sample 2 had some micro-particles. Since sample 2 also had messy networks, we thought with or without Ultra Sonic Vibrator did not change anything to the result.

Moving forward from sample 3 (Figure 19) to 7 (Figure 23) and also sample 12 (Figure 24), totally are six samples.

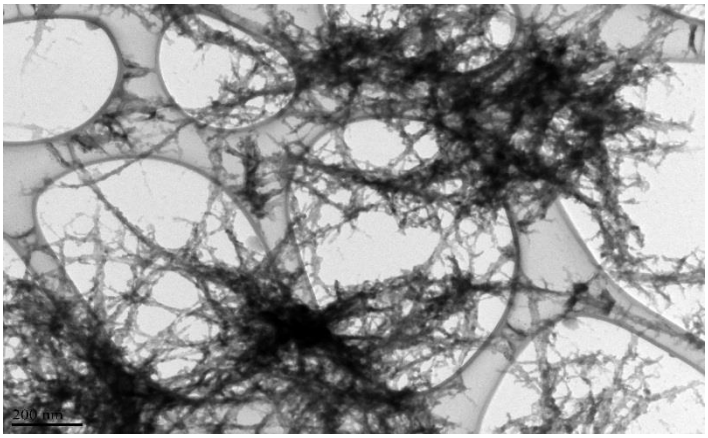

Figure 19
Sample 3
No ultrasonic vibrator
With E field set as 200V
Electrodes outside container
Water

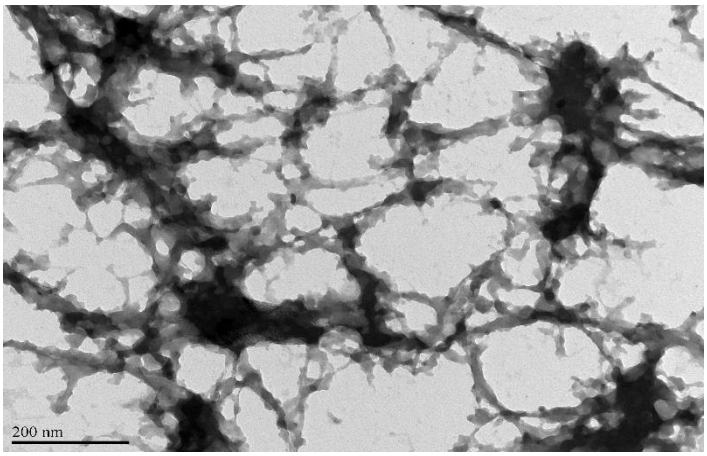

Figure 20
Sample 4
No ultrasonic vibrator
With E field set as 750V
Electrodes outside container
Water

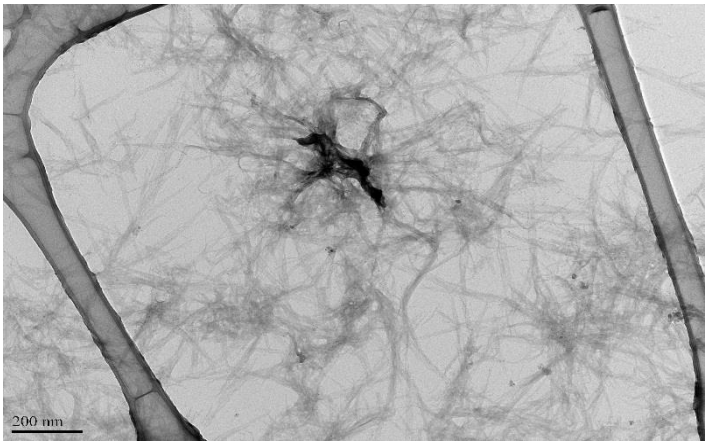

Figure 21
Sample 5
No ultrasonic vibrator
With E field set as 1000V
Electrodes outside container
Water

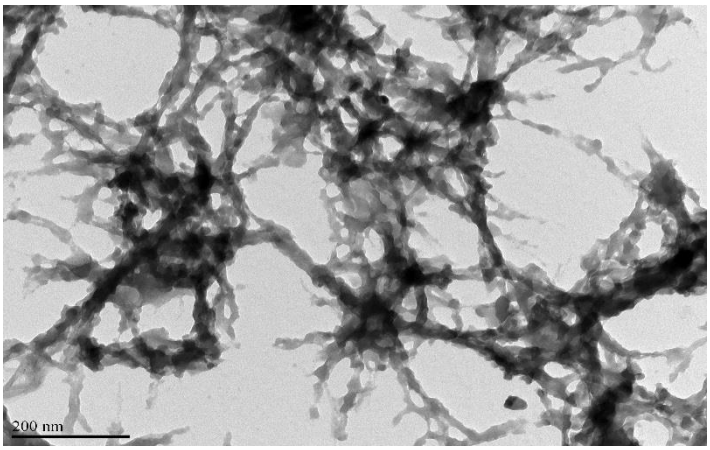

Figure 22
Sample 6
No ultrasonic vibrator
With E field set as 1500V
Electrodes outside container
Water

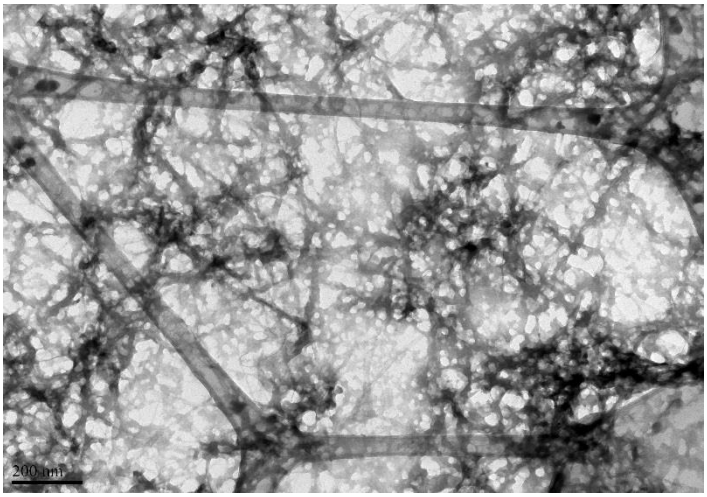

Figure 23
Sample 7
No ultrasonic vibrator
With E field set as 2000V
Electrodes outside container
Water

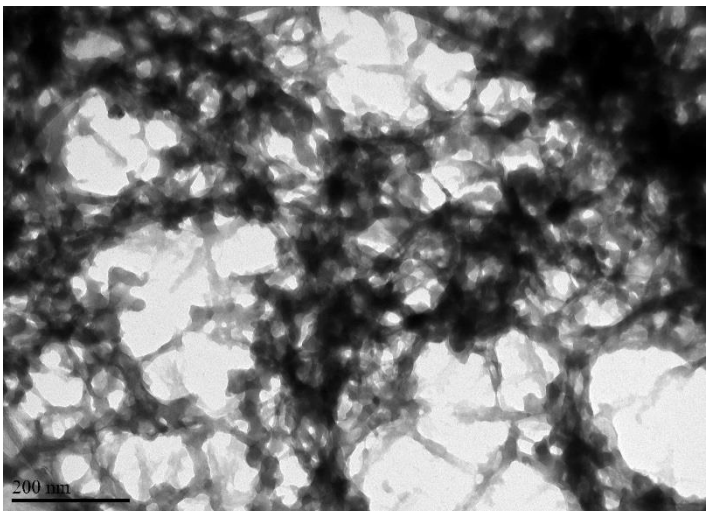

Figure 24
Sample 12
No ultrasonic vibrator
With E field set as 18V
Electrodes outside container
Water

Figure 19 to 24 are images of samples that were ablated in an electric field, with the electrodes outside of the container. The electrode distance was held constant at 24 mm however the E field was varied by changing the potential different between the electrodes (6 different volts 18V, 200V, 750V, 1000V, 1500V and 2000V). From the previous images we see that the ablated material forms messy networks with no significant dependence of the morphology on the electric field. Based on this, it was concluded when the electrodes outside the container, the changing of voltage would not influence the result.

We also conducted experiments with the electrodes inside the container. In this configuration the electrode separation was 19 mm.

Samples 8 and 9 were both ablated under electrodes that had an 18 V potential difference, however the samples were dried differently to see what impact that has on the final product.

By using the dry system, sample 8 was dried by leaving the vial containing 20ml and the nanoparticles in a fume hood and waiting the 3-4 days for the 20ml to evaporate. In contrast, sample 9 was kept on a hotplate at 60 ^{o}C and all of the liquid evaporated in approximately 90 minutes. Let's comparing samples 8 (Figure 25) and 9 (Figure 26).

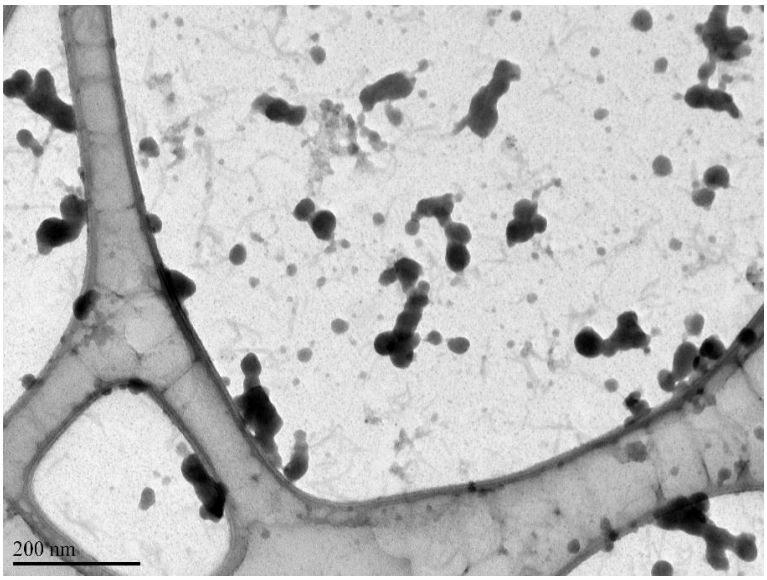

Figure 25
Sample 8
No ultrasonic vibrator
With E field set as 18V
Electrodes inside container
Water
Room temperature

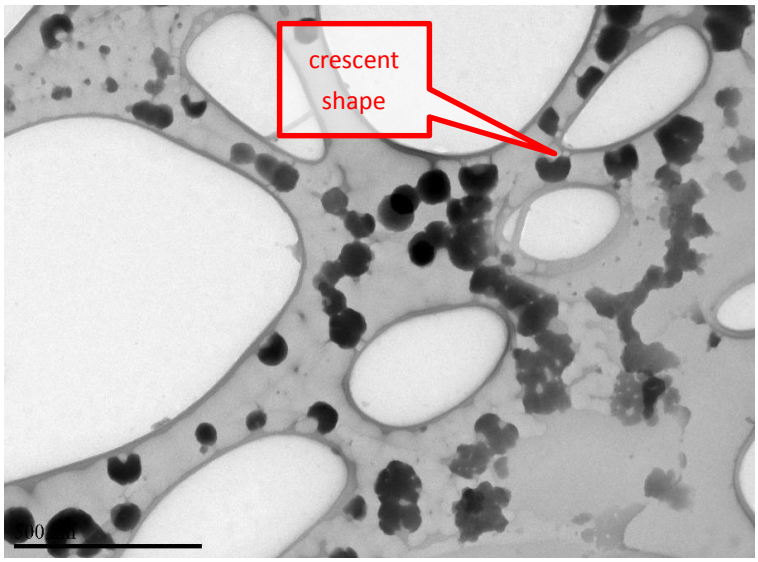

Figure 26
Sample 9
No ultrasonic vibrator
With E field set as 18V
Electrodes inside container
Water
60 ^{o}C

Both images have around 30 nm size nanoparticles. However, the interesting difference is that there are some crescent shaped nanoparticles in sample 9, the sample dried quickly. We speculate this might be caused by bubbles inside the liquid, while they break when the germanium nanoparticles are drying, although we cannot now confirm this idea. I was more interested in the impact of the electric field so did not pursue this, however in the future it may be worth the impact of different drying techniques on the

resulting nanoparticles.

Compared sample 2 (Figure 18) with sample 8 (Figure 25), it shows us the obvious changing is the size of the particles. With increasing of E field, the size of the particles

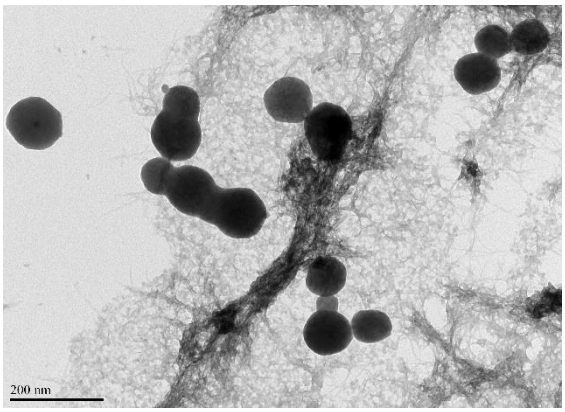

Figure 18
Sample 2
No ultrasonic vibrator
No E field
Water

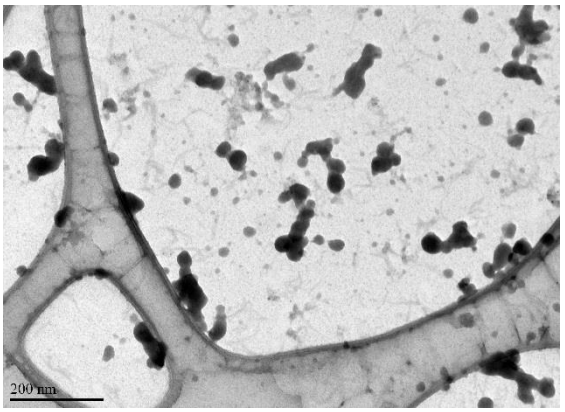

Figure 25
Sample 8
No ultrasonic vibrator
With E field set as 18V
Electrodes inside container
Water

from micro level particles dropped down to 30nm nanoparticles. Since the only difference between these two samples are E field (0V for sample2, 18V for sample 8), we guess the changing of the E field might influence the ablated result.

We tried to use ethanol instead of distilled water then followed the same experiment procedures as sample 2 and sample 8, the similar phenomenon presented when we compared sample 10 (0V, figure 27) and sample 11 (18V, figure 28):

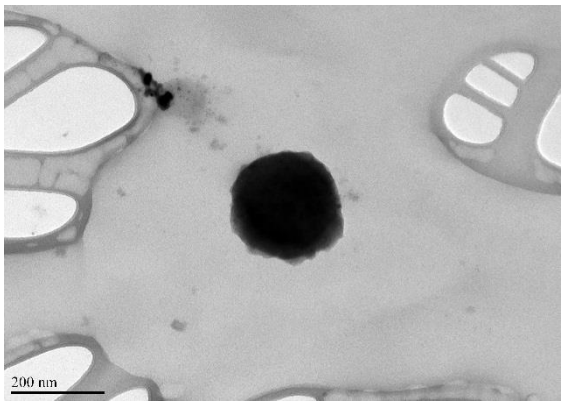

Figure 27
Sample 10
No ultrasonic vibrator
No E field
Ethanol

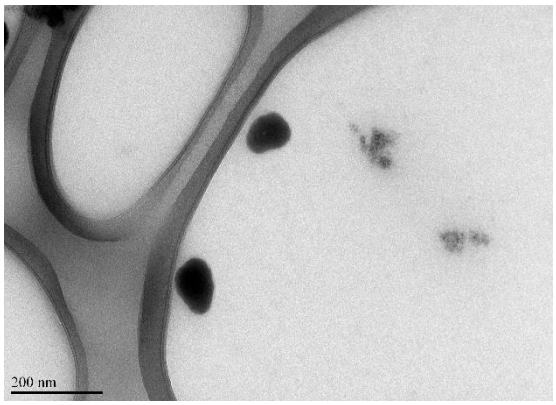

Figure 28
Sample 11
No ultrasonic vibrator
With E field set as 18V
Electrodes inside container
Ethanol

from the above images we can see even in the ethanol with different set of the electric field, the average size of particles in these two images are different too. In sample 10, the particle size is around 200nm and it is around 80nm in sample 11. After comparing sample 2 and sample 8, also sample 10 and sample 11, we boldly conjecture that: the stronger electric field, the smaller size of the particles.

Additional experiments were performed to conclude our original results, thus sample 13 to sample 32. Germanium was ablated at 5 different voltages (0V, 5V, 10V, 15V, 18V), while keeping other parameters as constant. And the liquid still distilled water or ethanol. After getting enough images from all the samples, the next step is going to measure the size of particles in each electric field.

Software “Paint” had been used to do the measuring work. First of all, figure out the pixel of the scale on the image. Then get the pixel size for each particle, then use the following equation to measure the size of each particle:

$$\text{Particle Size} = \frac{PX_p \times L}{PX_s} \quad (4.1)$$

Where PX_p is the pixel of the particle; PX_s is the pixel of the scale; L is the length of the scale that shows on the images (200nm here). Schematic picture shows below (Figure 29):

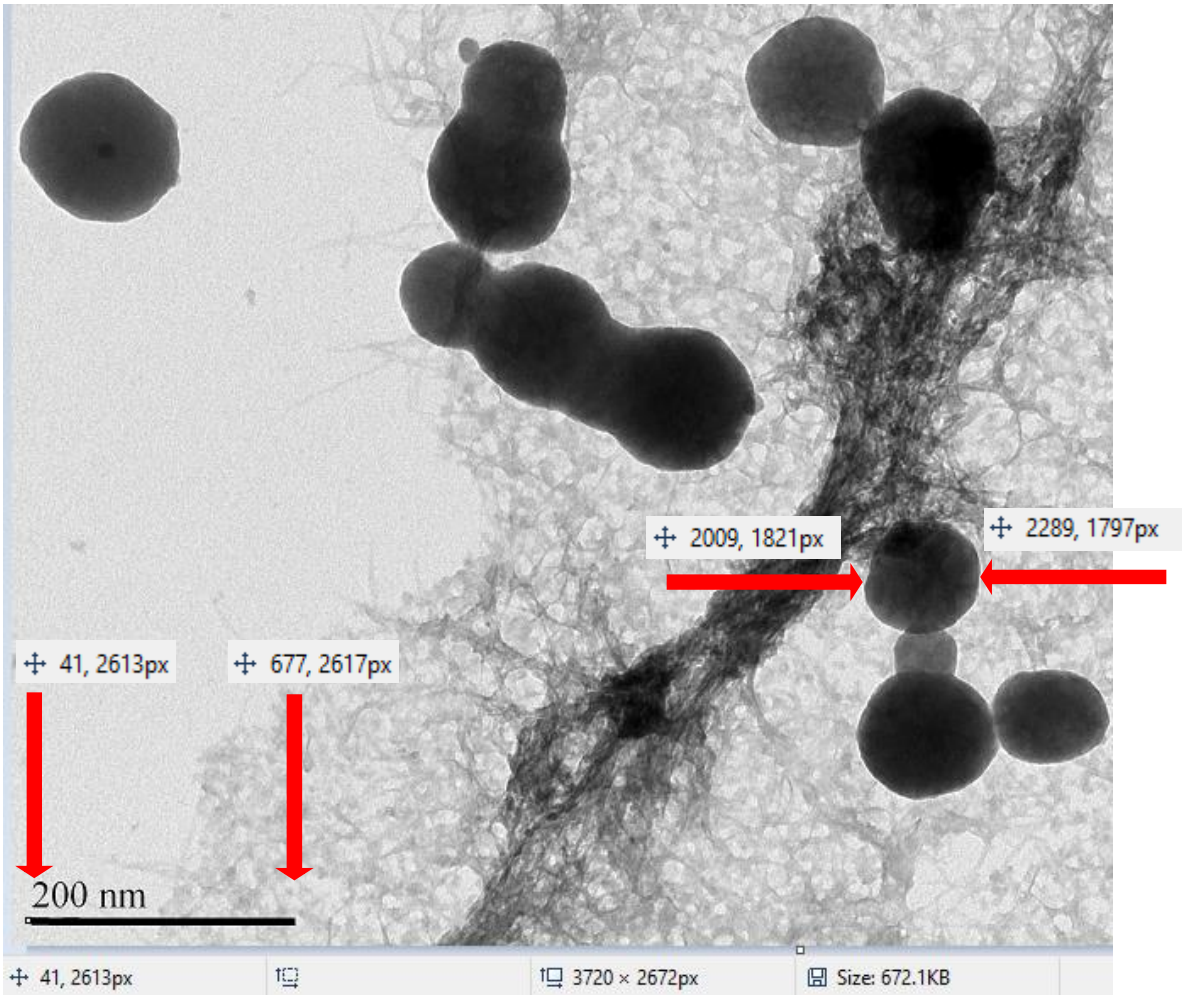

Figure 29 for Sample 2, which is no ultrasonic vibrator, no E field and ablated in water.

For example, from above image the pixel of scale is PX_p=677-41=636; the pixel of particle is PX_s=2289-2009=280; L=200nm; put the number into equation (4.1) and the particle size of this marked particle is 88nm. Using this method to measure each particles in this image and calculate the average size, standard deviation of these

particles. Collecting average particle size, standard deviation from five different externally applied electric fields and different immerse liquids; then made a graph of all the data (Figure 30):

From this graph, we can see the average particle size decreased while the externally

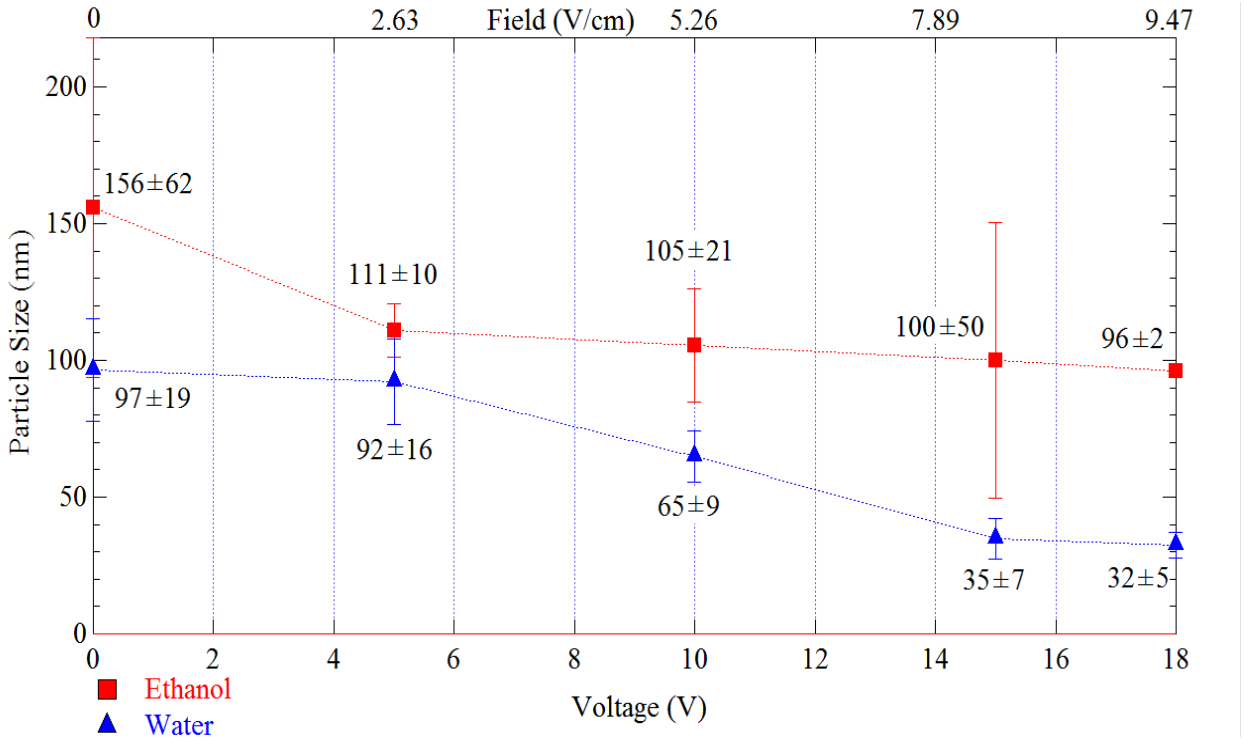

Figure 30 Particle size – Voltage/Field graph. Shows the relationship between different electric fields and the average particle size.

applied electric field is increased. When the laser ablation happened in distilled water, the average particle size dropped 67% from 0V/cm to 9.47V/cm electric field, for ethanol, it had dropped 38% from 0V/cm to 9.47V/cm electric field. This result confirmed our previous suspect about the externally applied electric field influences.

CHAPTER 5
CONCLUSION

5.1 Conclusion

From the results from our experiment we can draw the following conclusions from laser ablation of germanium in water and ethanol:

(1). All things being equal, ablation in water results in smaller nanoparticles than ablation in ethanol.

(2). Different drying techniques, one at room temperature, and another at 60^{o}C, had no observable impact on particle size and a small impact on morphology, with rapid heating producing some crescent shaped nanoparticles.

(3). Ultrasonic vibration during ablation prevents formation of nanoparticles with sizes of ~ 10 nm. Instead, a nano-mesh was made.

(4). Externally applied electric fields have no impact on nanoparticle formation when the electrodes are placed outside of the container.

(5). When the electrodes are placed inside of the container, there is a clear correlation of decreasing particle size with increasing externally applied electric field.

BIBLIOGRAPHY

1. H. Zeng, X. W. Du, S. C. Singh, S. A. Kulinich, S. Yang, J. He and W. Cai, Advanced Functional Materials **22** (7), 1333-1353 (2012).

2. Peter W. Milonni and J. H. Eberly, *LASERS*, 1 ed. (Wiley, John & Sons, Incorporated, November, 1988).

3. M. Hoffmann, Met Constr **11** (1), 33-34 (1979).

4. A. V. Simakin, V. V. Voronov and G. A. Shafeev, Physics of Wave Phenomena **15** (4), 218-240 (2007).

5. Y. Iida, A. Tsuge, Y. Uwamino, H. Morikawa and T. Ishizuka, Journal of Analytical Atomic Spectrometry **6** (7), 541-544 (1991).

6. G. W. Yang and J. B. Wang, Applied Physics A: Materials Science and Processing **71** (3), 343-344 (2000).

7. R. Nyga and W. Neu, Optics Letters **18** (9), 747-749 (1993).

8. D. Garza, G. Grisel Garc á, M. I. Mendivil Palma, D. Avellaneda, G. A. Castillo, T. K. Das Roy, B. Krishnan and S. Shaji, Journal of Materials Science **48** (18), 6445-6453 (2013).

9. C. Niu, Y. Z. Lu and C. M. Lieber, Science **261** (5119), 334-337 (1993).

10. A. M. Van Der Valk, Drug Discovery Today **8** (17), 781-783 (2003).

11. D. Y. H. Pui and D. R. Chen, Journal of Aerosol Science **28** (4), 539-544 (1997).

12. B. K. Sinha and N. Gopi, Applied Physics Letters **35** (1), 11-13 (1979).

13. J. T. Cheung and H. Sankur, Critical Reviews in Solid State and Materials Sciences **15** (1), 63-109 (1988).

14. D. J. Lichtenwalner, O. Auciello, R. Dat and A. I. Kingon, Journal of Applied Physics **74** (12), 7497-7505 (1993).

15. H. Izumi, K. Ohata, T. Morishita and S. Tanaka, IEEE Transactions on Magnetics **27** (2 pt II), 1449-1452 (1991).

16. S. E. Black, *Laser ablation : effects and applications*. (Nova Science Publishers, Hauppauge, N.Y., 2011).

17. T. E. Itina, The Journal of Physical Chemistry C **115** (12), 5044-5048 (2010).

18. S. A. Darke, S. E. Long, C. J. Pickford and J. F. Tyson, Journal of Analytical Atomic Spectrometry **4** (8), 715-719 (1989).

19. P. P. Patil, D. M. Phase, S. A. Kulkarni, S. V. Ghaisas, S. K. Kulkarni, S. M. Kanetkar, S. B. Ogale and V. G. Bhide, Physical Review Letters **58** (3), 238-241 (1987).

20. G. W. Yang, Progress in Materials Science **52** (4), 648-698 (2007).

21. S. M. Hamidi, M. A. Oskuei, S. Sadeghi and M. M. Tehranchi, Journal of Superconductivity and Novel Magnetism, 1-4 (2013).

22. P. Liu, H. Cui, C. X. Wang and G. W. Yang, Physical Chemistry Chemical Physics **12** (16), 3942-3952 (2010).

23. H. S. Park, S. H. Nam and S. M. Park, in *EIGHTH INTERNATIONAL CONFERENCE ON LASER ABLATION (COLA'05)* (Journal of Physics: Conference Series, Banff, Canada, 2007), Vol. 59.

24. S. Bhattacharyya, S. S. N. Bharadwaja and S. B. Krupanidhi, Journal of Applied Physics **88** (7), 4294-4302 (2000).

25. P. Liu, C. X. Wang, X. Y. Chen and G. W. Yang, Journal of Physical Chemistry C

112 (35), 13450-13456 (2008).

26. N. G. Basov, V. A. Danilychev, Y. U. M. Popov and D. D. Khodkevich, JETP Lett **12** (10), 329-331 (1970).

27. C. R. Munnerlyn, S. J. Koons and J. Marshall, Journal of Cataract and Refractive Surgery **14** (1), 46-52 (1988).

28. I. G. Pallikaris and D. S. Siganos, Journal of Refractive and Corneal Surgery **10** (5), 498-510 (1994).

29. J. R. Lankard Sr and G. Wolbold, Applied Physics A Solids and Surfaces **54** (4), 355-359 (1992).

30. M. Koch, S. Rehbein, G. Schmahl, T. Reisinger, G. Bracco, W. E. Ernst and B. Holst, Journal of Microscopy **229** (1), 1-5 (2008).

31. D. B. Williams and C. B. Carter, *Transmission Electron Microscopy: A Textbook for Materials Science*, second ed. (Springer, 2009).

32. D. E. N. Joseph Goldstein, D C. Joy, C E. Lyman, P Echlin, E LIfshin, L Sawyer, and J R. Michael., *Scanning Electron Microscopy and X-ray Microanalysis*, (3 ed) ed. (Springer, 2003).

33. *电动力学*. (高等教育出版社, 2004).

34. J. D. Jackson, *Classical Electrodynamics*. (Wiley, 1999).

35. N. M. Bulgakova and A. V. Bulgakov, Applied Physics A **73** (2), 199-208 (2001).

36. X. Xu, Applied Surface Science **197-198**, 61-66 (2002).

37. R. Clausius, Mathematische Annalen **4** (2), 231-242 (1871).

38. M. D. Lechner and C. Wohlfarth, in *Supplement to IV/18* (Springer Berlin

Heidelberg, 2009), Vol. 25, pp. 110-120.

VITA

Yilu Li was born on May 12th, 1988, in Nanjing, Jiangsu Province of P.R.China. In 2010, he graduated from Changchun University of Science and Technology and received the Bachelor degree of Science. After a short work, in August 2011, he moved to United States for his higher education. He is currently pursuing his Masters in Physics at the University of Missouri – Kansas City. He will continue his Ph.D. study in University of Missouri – Kansas City.

He worked as a Graduate Teaching Assistant in Physics Department since January 2012. He joined Condensed Matter Physics Group of Prof. Kruger in June 2012 and started his physics research career. Through the period of research, he worked with Post Doctoral Reasercher Omar Musaev on the project about laser ablation. In September 2013, he presented a poster titled “Laser ablation of Ge in liquid in electric field”at 57th Midwest Solid State Conference that is held by University of Kansas, Lawrence, KS.